

# We are IntechOpen, the world's leading publisher of Open Access books Built by scientists, for scientists

6,900

Open access books available

186,000

International authors and editors

200M

Downloads

Our authors are among the

154

Countries delivered to

TOP 1%

most cited scientists

12.2%

Contributors from top 500 universities



WEB OF SCIENCE™

Selection of our books indexed in the Book Citation Index  
in Web of Science™ Core Collection (BKCI)

Interested in publishing with us?  
Contact [book.department@intechopen.com](mailto:book.department@intechopen.com)

Numbers displayed above are based on latest data collected.  
For more information visit [www.intechopen.com](http://www.intechopen.com)



## MATLAB: A Systems Tool for Design of Fuzzy LMI Controller in DC-DC Converters

Carlos Andrés Torres-Pinzón and Ramon Leyva  
*Department of Electronic, Electrical, and Automatic Control Engineering  
 Rovira i Virgili University  
 Tarragona, Spain*

### 1. Introduction

DC-DC switching converters are devices usually used to adapt primary energy sources to the load requirements (Erickson & Macksimovic, 2001). These devices produce a regulated output voltage despite changes in the feed voltage or in the load current. There are three basic topologies of dc-dc converters, namely the buck, the boost and the buck-boost converter. The buck converter is used to reduce output voltage, while the boost converter increase the output voltage. In the buck-boost converter, the output voltage can be maintained either higher or lower than the source but in the opposite polarity. These basic converters consist of two reactive elements; namely, an inductor and a capacitor, besides a transistor and a diode to perform the commutation, the size of reactive elements are chosen to guarantee a low level of ripple and hence an averaged dynamical model behavior is a good approximation of the switched behavior.

In order to maintain a regulated output and to have a damped enough response some control loops are added to command the converter. The signal which drives the transistor used to be a squared, constant-period and high frequency signal.

The design of the control loops is commonly based on linearized dynamic models around equilibrium point of the converter (Erickson & Macksimovic, 2001). Nevertheless, commonly the averaged dynamical models of these plants are nonlinear and their linearization is non minimum phase. Therefore, using linear controllers can only ensures stability and dynamic performances around equilibrium point, and hence, instabilities or bad performances may appear when large signal perturbations occur. This fact has prompted several authors to apply nonlinear control methods to regulate switching converters.

Some of the first researches on nonlinear controller design for dc-dc converters can be found in the studies of (Sanders & Verghese, 1992) and (Kawasaki et al., 1995). These authors propose non-linear strategies based on Lyapunov functions, which allows the converter to ensure stability over a wide range of operating conditions. More recent studies are those of (Leyva et al., 2006) and (He & Luo, 2006) which derive robust non-linear controller for large-signal stability in dc-dc converters and present efficient implementations.

Furthermore, robust control approaches have been applied in dc-dc converters which take into account nonlinearities and uncertainties (Olalla et al., 2009; 2010).

Another promising nonlinear technique for controlling power converters is the model-based fuzzy control technique. The model-based fuzzy approaches begin by constructing the

corresponding (T-S) Takagi–Sugeno fuzzy model representation of the nonlinear system (Tanaka & Wang, 2001). This T-S fuzzy representation is described by fuzzy rules IF-THEN which represent local linear input-output relations of the nonlinear plant. Once fuzzy rules are obtained with linear submodels, the control design is based on the technique known as Parallel Distributed Compensator (PDC), where each control rule is designed from the corresponding rule of the T-S fuzzy model (Korba et al., 2003). The stability analysis is carried out using Lyapunov functions on the closed-loop system. The Lyapunov functions are formulated into linear matrix inequalities (LMIs). This approach is fundamentally different from heuristics based fuzzy control (Tanaka & Wang, 2001) where the rules are based on heuristic knowledge. A model-based fuzzy control for dc-dc converters have been described in (Kuang et al., 2006), where the authors show a fuzzy law for the buck and ZVT buck converters. Other authors who applied this technique in dc-dc converters are (Lan & Tan, 2009)

Nowadays, thanks to the powerful computational tools and optimization techniques, many robust and fuzzy control designs based on LMIs can be readily solved. Matlab is a powerful tool in this process. The LMI Toolbox of Matlab is an efficient software tool based on interior point methods (Gahinet et al., 1995), which it can be used to numerically solve many LMI control problems that otherwise could not be solved since they have not an analytical solution. The main advantage of the LMI formulations is the ability to combine various design constraints and objectives in a numerically tractable manner.

This chapter presents a synthesis of LMI fuzzy controllers for dc-dc converters. The chapter describes in detail a compact control design methodology which takes into account constraints such as: control effort and the decay rate of state variables. The chapter is organized as follows: First, in section 2, we review the dynamics of a buck and a boost converter. In section 3, we introduce the T-S fuzzy representation of dc-dc converters, with their corresponding uncertainties. Aspects of the LMI fuzzy control design are explained in section 4. In section 5, we present two design examples to illustrate the advantages of the procedure. The first example shows the LMI controller of a buck converter, while in the second, we obtain an LMI Fuzzy controller for a boost converter working at different operating point. Both examples have been simulated with Matlab and the results are in perfect agreement with the design specification. Finally, we summarize the main ideas in section 6.

## 2. Modeling of DC-DC converters. A dynamical review

This section presents basic PWM converters and their state-space models which are used in the following sections. Specifically, the section describes the dynamic behavior of buck and boost converters.

### 2.1 Model of PWM buck converters

Fig.1 shows a dc-dc step-down (buck) converter, this power electronic stage reduces and regulates the output voltage from a primary voltage source.

The converter switch alternates periodically between two positions. Fig. 2 shows the circuits corresponding to *on* and *off* during intervals  $T_{on}$  and  $T_{off}$ , respectively. These positions are driven by the binary signal  $u$  whose values are  $u = 1$  during  $T_{on}$  and  $u = 0$  during  $T_{off}$ . The voltage reduction of this converter in steady state corresponds to the ratio  $T_{on}/T_s$ . We model the converter dynamics at each position by using the Kirchhoff laws. Its dynamic expressions

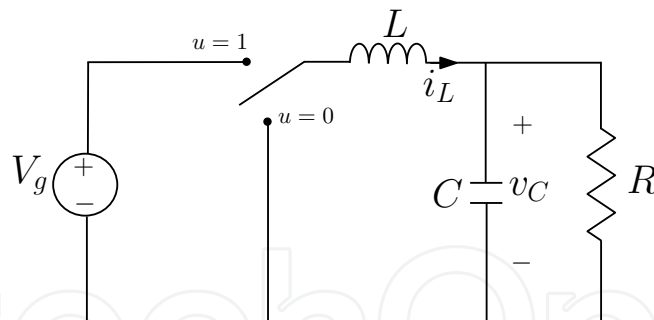


Fig. 1. Schematic circuit of a buck converter

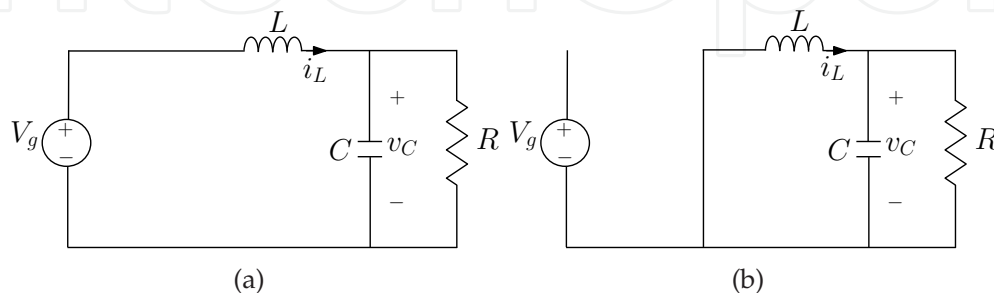


Fig. 2. Equivalent circuit during  $T_{on}$  (a) and  $T_{off}$  (b).

in state-space at each position correspond to

$$\begin{aligned} \dot{x}(t) &= A_{on}x(t) + B_{u_{on}} \quad \text{during } T_{on} \\ \dot{x}(t) &= A_{off}x(t) + B_{u_{off}} \quad \text{during } T_{off} \end{aligned} \quad (1)$$

being

$$A_{on} = A_{off} = \begin{bmatrix} 0 & -\frac{1}{L} \\ \frac{1}{C} & -\frac{1}{RC} \end{bmatrix} \quad B_{u_{on}} = \begin{bmatrix} \frac{V_g}{L} \\ 0 \end{bmatrix} \quad B_{u_{off}} = \begin{bmatrix} 0 \\ 0 \end{bmatrix} \quad (2)$$

and

$$x(t) = [i_L(t) \ v_C(t)]^T$$

where  $V_g$  is the feed voltage or primary source and  $v_C$  is the output voltage.  $R$  models the load, while  $L$  and  $C$  stand for inductance and capacitance values, respectively. The state vector  $x(t)$  consists of the inductor current  $i_L(t)$  and the capacitor voltage  $v_C(t)$ .  $A_{on}$  and  $B_{u_{on}}$  are the transition matrix and input vector, respectively, during  $T_{on}$  and  $A_{off}$  and  $B_{u_{off}}$  are the transition matrix and input vector during  $T_{off}$ .

The binary signal  $u$  turn on and off the switch which is controlled by means of a pulse width modulator (PWM), whose switching period  $T_s$  is equals to the sum of  $T_{on}$  and  $T_{off}$ . The PWM duty cycle is noted as  $d$ .

The expressions (1) and (2) can be written compactly in terms of the binary signal  $u$  as follows

$$\dot{x}(t) = A_{off}x(t) + B_{off} + (A_{on} - A_{off})xu + (B_{on} - B_{off})u \quad (3)$$

The converter operates in continuous conduction mode (CCM) when the inductor current  $i_L$  is ever greater than zero. We assume this operation mode then the switched model (3) can be

approximated using state-space averaging method (Middlebrook & Cuk, 1976), replacing the binary signal  $u$  by its respective duty cycle  $d$  and the state variables by their averaged values during the switching period. The result of this averaging process can be written as

$$\dot{\bar{x}}(t) = A_{off}\bar{x}(t) + B_{off} + (A_{on} - A_{off})\bar{x}d + (B_{on} - B_{off})d \quad (4)$$

Thus, the averaged state vector  $\bar{x}$  corresponds to  $\bar{x} = (\bar{i}_L, \bar{v}_C)^T$ ; where  $\bar{i}_L$  and  $\bar{v}_C$  are the averaged values of inductor current and capacitor voltage during a switching period.

Usually the bilinear model (4) is linearized around equilibrium point by considering that the system variables consist of two components:

$$\begin{aligned} \bar{x}(t) &= X + \hat{x}(t) \\ d(t) &= D + \hat{d}(t) \end{aligned} \quad (5)$$

where  $X$  and  $D$  represent the equilibrium values and  $\hat{x}$  and  $\hat{d}$  are the perturbed values of the state and duty cycle. Therefore, equation (4) can be written as follows

$$\dot{\hat{x}} = [A_{off} + (A_{on} - A_{off})D]\hat{x} + [(B_{on} - B_{off}) + (A_{on} - A_{off})X]\hat{d} \quad (6)$$

The equilibrium state in the buck converter corresponds to

$$X = \begin{bmatrix} \frac{V_g D}{R} \\ V_g D \end{bmatrix} \quad (7)$$

Taking into account (2), we can model the buck converter as

$$\dot{\hat{x}}(t) = \begin{bmatrix} 0 & -\frac{1}{L} \\ \frac{1}{C} & -\frac{1}{RC} \end{bmatrix} \hat{x}(t) + \begin{bmatrix} \frac{V_g}{L} \\ 0 \end{bmatrix} \hat{d}(t) \quad (8)$$

The model can be augmented to ensure zero steady-state error of  $v_C$  by introducing a new state variable  $x_3$  corresponding to

$$x_3(t) = \int (v_C(t) - V_{ref}) dt \quad (9)$$

where  $V_{ref}$  is the voltage reference.

Thus, the augmented model can be written as

$$\dot{\hat{x}}(t) = A\hat{x}(t) + B_u\hat{d}(t) \quad (10)$$

where

$$A = \begin{bmatrix} 0 & -\frac{1}{L} & 0 \\ \frac{1}{C} & -\frac{1}{RC} & 0 \\ 0 & 1 & 0 \end{bmatrix} \quad B_u = \begin{bmatrix} \frac{V_g}{L} \\ 0 \\ 0 \end{bmatrix} \quad (11)$$

In the next subsection, we develop the same procedure for the boost converter.

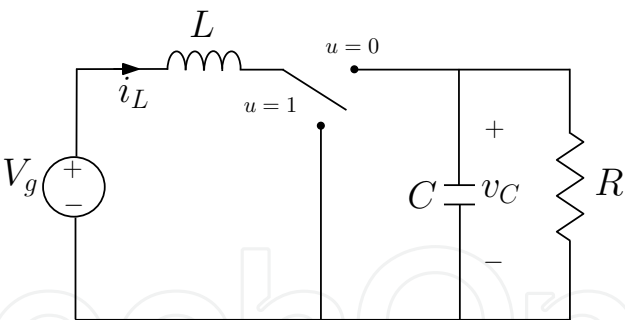


Fig. 3. Schematic circuit of a boost converter

2.2 Model of PWM boost converters

The Fig.3 shows the well-known boost converter (Erickson & Macksimovic, 2001), which is capable of regulating a dc output voltage when it is higher than the dc feed voltage. The dynamic behavior of boost converter during  $T_{on}$  and  $T_{off}$  shown in the Fig. 4 can be written as

$$A_{on} = \begin{bmatrix} 0 & 0 \\ 0 & -\frac{1}{RC} \end{bmatrix} \quad A_{off} = \begin{bmatrix} 0 & -\frac{1}{L} \\ \frac{1}{C} & -\frac{1}{RC} \end{bmatrix} \quad B_{u_{on}} = B_{u_{off}} = \begin{bmatrix} \frac{V_g}{L} \\ 0 \end{bmatrix} \tag{12}$$
$$x(t) = [i_L(t) \ v_C(t)]^T$$

where  $x(t)$  is the state-space vector composed of  $i_L$ , which represents the inductor current, and  $v_C$ , which represents the capacitor voltage. These variables are measurable and available for feedback purposes.

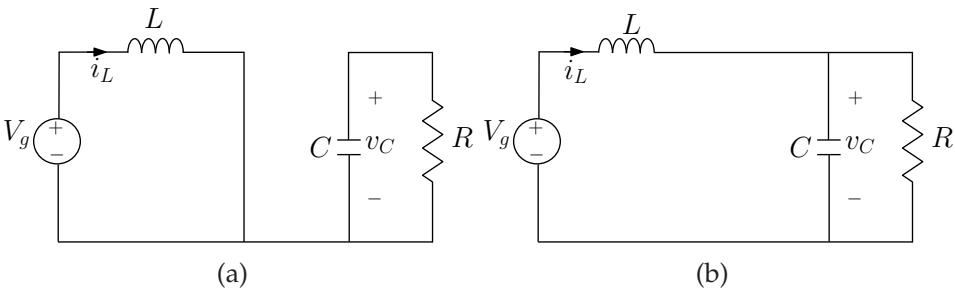


Fig. 4. Equivalent circuit of boost converter for  $T_{on}$  (a) and  $T_{off}$  (b).

Therefore, according to (12), the equilibrium state in the boost converter corresponds to

$$X = \begin{bmatrix} \frac{V_g}{RD'^2} \\ \frac{V_g}{D'} \end{bmatrix} \tag{13}$$

where  $D' = 1 - D$  is the complementary steady-state duty-cycle. Since  $A_{on} \neq A_{off}$ , the average model of the boost converter is bilinear, which can be written as:

$$\dot{\hat{x}} = A\hat{x} + B_u(\hat{x})\hat{d} \tag{14}$$

being

$$A = \begin{bmatrix} 0 & -\frac{D'}{L} & 0 \\ \frac{D'}{C} & -\frac{1}{RC} & 0 \\ 0 & 1 & 0 \end{bmatrix} \quad B_u(\hat{x}) = \begin{bmatrix} \frac{V_g}{D'L} + \frac{\hat{v}_C(t)}{L} \\ -\frac{V_g}{(D'^2R)C} - \frac{\hat{i}_L(t)}{C} \\ 0 \end{bmatrix} \tag{15}$$

In next section, we describes the T-S fuzzy modeling method for the DC-DC converters.

### 3. Takagi-Sugeno fuzzy representation of DC-DC converters

There exist several approaches to fuzzy representation of dynamic systems, between them the most common are the Mamdani fuzzy representation (Driankov et al., 1993) and the T-S fuzzy representation (Tanaka & Wang, 2001). In the first representation, it is assumed that there is no model of the plant, while the second representation is always based on a dynamical model of the plant.

This T-S representation describes the dynamic system by means of an interpolation of linear submodels. The performance requirements of a linear model may be expressed by means of LMI.

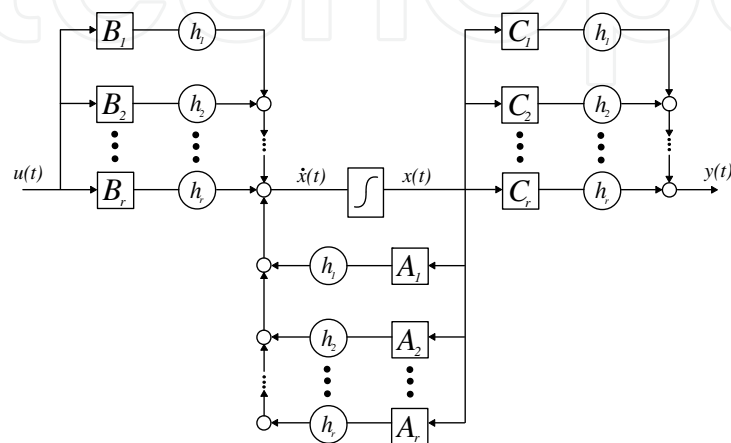


Fig. 5. Final structure of the Takagi-Sugeno fuzzy model

Figure 5 shows the model of the nonlinear plant as a group of linear models, which locally represent the relationship input-output system (Takagi & Sugeno, 1985), described of the form:

$$R_i : \text{If } \delta_1 \text{ is } M_{i1} \text{ and } \dots \text{and } \delta_j \text{ is } M_{ji} \text{ then} \\ \dot{x}_i(t) = A_i x(t) + B_i u(t) \quad i = 1, 2, \dots, r \quad (16)$$

Where  $r$  is the number of submodels,  $A_i$  is the system matrix of the  $i$ -th linear submodel,  $B_i$  is the input matrix,  $x(t)$  is the global state-space vector,  $u(t)$  is the input vector,  $M_{ji}$  are fuzzy sets, and  $\delta_j$  is the scheduling vector (Korba et al., 2003).

Fuzzy sets  $M_{ji}$  have associated membership functions  $\eta$ 's which characterize the degree of membership (Takagi & Sugeno, 1985). The nonlinearities of the plant will determine the variables of the scheduling vector  $\delta_i$  used in the antecedent, i.e., a correct election of scheduling variables will capture all the nonlinearities of the plant, in the case of the dc-dc converters the scheduling variables are function of the state variables  $\delta(t) = \delta(x(t))$  (Korba et al., 2003; Tanaka & Wang, 2001). The entire fuzzy model of the plant corresponds to a fuzzy weighting of the locally valid linear submodel associated to each implications  $R_i$  (Korba et al., 2003), i.e.,

$$\dot{x}(t) = \frac{\sum_{i=1}^r w_i(\delta(t)) [A_i x(t) + B_i u(t)]}{\sum_{i=1}^r w_i(\delta(t))} \quad (17)$$

Weights  $w_i(\delta(t))$  are zero or positive time-variant values and the sum of all the weights is positive.



$$\sum_{i=1}^r w_i(\delta(t)) > 0, \quad w_i(\delta(t)) \geq 0 \quad \forall \quad i = 1, 2, \dots, r$$

We use the next normalized weight function  $h_i(\delta(t))$  replacing  $w_i(\delta(t))$ ,

$$h_i(\delta(t)) = \frac{w_i(\delta(t))}{\sum_{i=1}^r w_i(\delta(t))}$$

that fulfill with

$$0 \leq h_i(\delta(t)) \leq 1, \quad \sum_{i=1}^r h_i(\delta(t)) = 1 \quad (18)$$

Therefore the fuzzy model (17) can be rewritten as

$$\dot{x}(t) = \sum_{i=1}^r h_i(\delta(t)) [A_i x(t) + B_i u(t)] \quad (19)$$

The T-S fuzzy model of the buck converter is expressed by only one rule given that it is linear. The T-S fuzzy models of other topologies require several rules given that their dynamic behaviour is bilinear. The boost converter case is shown in the next subsection.

### 3.1 Takagi-Sugeno model of a boost converter

We propose the next boost converter fuzzy model consisting of the following four rules.

- **R<sub>1</sub>:**

$$\begin{aligned} &\text{If } \hat{i}_L \text{ is } i_{small} \text{ and } \hat{v}_C \text{ is } v_{small} \text{ then} \\ &\quad \dot{\hat{x}}_1(t) = A_1 \hat{x}(t) + B_1 \hat{d}(t) \end{aligned} \quad (20)$$

- **R<sub>2</sub>:**

$$\begin{aligned} &\text{If } \hat{i}_L \text{ is } i_{big} \text{ and } \hat{v}_C \text{ is } v_{small} \text{ then} \\ &\quad \dot{\hat{x}}_2(t) = A_2 \hat{x}(t) + B_2 \hat{d}(t) \end{aligned} \quad (21)$$

- **R<sub>3</sub>:**

$$\begin{aligned} &\text{If } \hat{i}_L \text{ is } i_{small} \text{ and } \hat{v}_C \text{ is } v_{big} \text{ then} \\ &\quad \dot{\hat{x}}_3(t) = A_3 \hat{x}(t) + B_3 \hat{d}(t) \end{aligned} \quad (22)$$

- **R<sub>4</sub>:**

$$\begin{aligned} &\text{If } \hat{i}_L \text{ is } i_{big} \text{ and } \hat{v}_C \text{ is } v_{big} \text{ then} \\ &\quad \dot{\hat{x}}_4(t) = A_4 \hat{x}(t) + B_4 \hat{d}(t) \end{aligned} \quad (23)$$

where

$$A_1 = A_2 = A_3 = A_4 = A = \begin{bmatrix} 0 & -\frac{D'}{L} & 0 \\ \frac{D'}{C} & -\frac{1}{RC} & 0 \\ 0 & 1 & 0 \end{bmatrix}$$



$$\begin{aligned} B_1 &= \begin{bmatrix} \frac{V_g}{D'L} + \frac{v_{min}}{L} \\ -\frac{V_g}{(D'^2R)C} - \frac{i_{min}}{C} \\ 0 \end{bmatrix} & B_2 &= \begin{bmatrix} \frac{V_g}{D'L} + \frac{v_{min}}{L} \\ -\frac{V_g}{(D'^2R)C} - \frac{i_{max}}{C} \\ 0 \end{bmatrix} \\ B_3 &= \begin{bmatrix} \frac{V_g}{D'L} + \frac{v_{max}}{L} \\ -\frac{V_g}{(D'^2R)C} - \frac{i_{min}}{C} \\ 0 \end{bmatrix} & B_4 &= \begin{bmatrix} \frac{V_g}{D'L} + \frac{v_{max}}{L} \\ -\frac{V_g}{(D'^2R)C} - \frac{i_{max}}{C} \\ 0 \end{bmatrix} \end{aligned} \tag{24}$$

being the membership function of the fuzzy sets  $i_{small}, i_{big}, v_{small}$  and  $v_{big}$  the following ones,

$$\begin{aligned} \eta_{i_{small}}(\hat{i}_L) &= \frac{i_{max}-\hat{i}_L}{i_{max}-i_{min}} & \eta_{i_{big}}(\hat{i}_L) &= 1 - \eta_{i_{small}}(\hat{i}_L) \\ \eta_{v_{small}}(\hat{v}_C) &= \frac{v_{max}-\hat{v}_C}{v_{max}-v_{min}} & \eta_{v_{big}}(\hat{v}_C) &= 1 - \eta_{v_{small}}(\hat{v}_C) \end{aligned} \tag{25}$$

Note that (20) correspond to the dynamic behavior around  $(i_{min}, v_{min})$  values, and (21)-(23) describe the local behavior around the other interval bounds. Thus, the normalized weight functions are

$$\begin{aligned} h_1(\hat{i}_L, \hat{v}_C) &= \eta_{i_{small}} \cdot \eta_{v_{small}} & h_3(\hat{i}_L, \hat{v}_C) &= \eta_{i_{small}} \cdot \eta_{v_{big}} \\ h_2(\hat{i}_L, \hat{v}_C) &= \eta_{i_{big}} \cdot \eta_{v_{small}} & h_4(\hat{i}_L, \hat{v}_C) &= \eta_{i_{big}} \cdot \eta_{v_{big}} \end{aligned} \tag{26}$$

therefore the entire fuzzy converter model corresponds to

$$\dot{\hat{x}}(t) = \sum_{i=1}^r h_i(\hat{i}_L, \hat{v}_C) \left( A_i \hat{x}(t) + B_i \hat{d}(t) \right) \tag{27}$$

since  $\sum_{i=0}^r h_i = 1$  and  $A_i = A$  then

$$\dot{\hat{x}}(t) = A \hat{x}(t) + \left( \sum_{i=1}^r h_i(\hat{i}_L, \hat{v}_C) B_i \right) \hat{d}(t) \tag{28}$$

and it is worth to remark that (28) corresponds with the bilinear model (14) inside the polytope region  $[\hat{i}_{min}, \hat{i}_{max}] \times [\hat{v}_{min}, \hat{v}_{max}]$ . This operating space is depicted in Fig. (6).

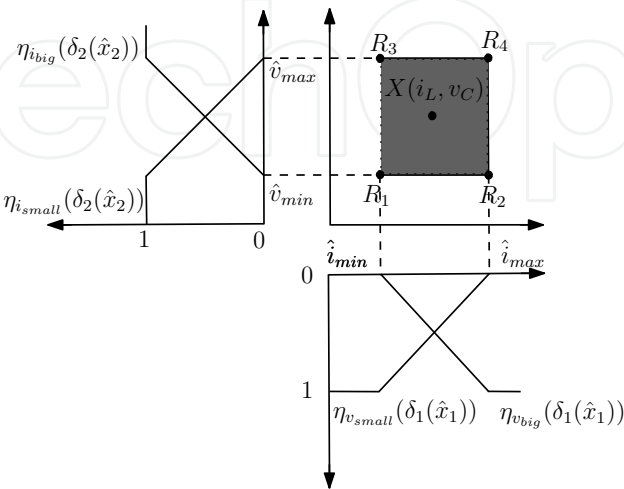


Fig. 6. T-S Fuzzy representation of the boost converter consisting of the 4 rules

The approach shown here can be easily adapted for the buck-boost converter, such as shown in (Torres-Pinzón & Leyva, 2009).

In next section, we explain a control strategy where the law consist of a normalized weight sum of linear feedback gains at each interval limit, which takes into account constraints such as: control effort and the decay rate of state variables.

#### 4. LMI performance requeriments

This section presents the concept and basic procedure of the parallel distributed compensation (PDC) technique and the definitions and LMI constraints used in the synthesis of control. First, we introduce the basic concept of Lyapunov-based stability. Then, we discuss on stability concepts for fuzzy systems in form of LMI. These concepts will be applied in Section 5 to find a LMI fuzzy controller for the buck and boost converters. It can be observed that since the buck converter dynamics is linear, we obtain a linear control law for this converter that is a fuzzy controller with only one rule.

##### 4.1 Quadratic stability conditions

Given the linear dynamic system

$$\dot{x}(t) = Ax(t) \quad (29)$$

the existence of a quadratic function of the form

$$V(x(t)) = x(t)^T Px(t) \quad (30)$$

that satisfies  $\dot{V}(x(t)) < 0$ , is a necessary and sufficient condition to ensure that the system is asymptotically stable, i.e., all trajectories converge to zero. Where  $P$  is a symmetric positive definite matrix  $\in \mathbb{R}^{n \times n}$ . Since the expression  $\dot{V}(x(t)) < 0$  has form quadratic, this condition is referred as quadratic stability, and it can be rewritten as follows

$$\dot{V}(x(t)) = x(t)^T (A^T P + PA) x(t) \quad (31)$$

Thus, the system is asymptotically stable if and only if there exist a symmetric matrix  $P$  such that

$$A^T P + PA < 0 \quad (32)$$

The main interest of the quadratic stability condition is that by means of a convex envelope and numerically simple test, it is possible to conclude about the overall stability of a dynamics system.

For an in-deep explanation on quadratic stability see (Boyd et al., 1994).

Based on the results (32), the following subsection present some basic results on the stability of fuzzy control systems.

##### 4.2 Performance constraints

In this subsection, we review in detail the Parallel Distributed Compensation (PDC) technique (Tanaka & Wang, 2001). In such fuzzy technique, each control rule is associated with the corresponding rule of the fuzzy model, thus the controller rules are as follows,

$$R_i : \text{If } \delta_1 \text{ is } M_{i1} \text{ and } \dots \text{ and } \delta_j \text{ is } M_{ji} \text{ Then}$$

$$u(t) = -F_i x(t) \quad i = 1, \dots, r \quad (33)$$

where  $F_i$  are lineal feedback gain vectors associate with each rule. And the overall fuzzy controller is represented as

$$u(t) = -\frac{\sum_{i=1}^r w_i F_i x(t)}{\sum_{i=1}^r w_i} = -\sum_{i=1}^r h_i F_i x(t) \quad (34)$$

Substituting the control law (34) in the fuzzy model (19), the closed loop system dynamics is given by

$$\dot{x}(t) = \sum_{i=1}^r \sum_{j=1}^r h_i h_j (A_i - B_i F_j) x(t) \quad (35)$$

In order to select the suitable feedback gain vectors  $F_i$ , we impose Lyapunov stability constraints and performance constraints on decay rate and control effort in form of LMIs.

Therefore, the sufficient conditions for the stability of the open-loop fuzzy system (19) and closed-loop one (35) are obtained using quadratic stability condition of the equation (32). These conditions, derived from (Tanaka & Wang, 2001), it can be expressed by means of the next propositions.

**Proposition 4.1.** *The equilibrium of the continuous fuzzy system (19) with  $u(t) = 0$  is asymptotically stable if there exists a common positive definite matrix  $P$  such that*

$$\begin{aligned} A_i^T P + P A_i &< 0, \quad i=1, \dots, r \\ P &> 0 \end{aligned} \quad (36)$$

that is, a common  $P$  has to exist for all subsystems

where  $A_i$  are system matrices of the linear submodels defined in the previous section.

**Proposition 4.2.** *The equilibrium of the continuous fuzzy control system described by (35) is asymptotically stable if there exists a common positive definite matrix  $P$  such that*

$$\begin{aligned} (A_i - B_i F_j)^T P + P (A_i - B_i F_j) &< 0, \quad j > i \\ P &> 0 \end{aligned} \quad (37)$$

Note that the condition (37) is not linear because involves the multiplication of the variables  $P$  and  $F_j$ 's. Thus, in order to rewrite (37) in a linear manner, we multiply the inequality (37) on the left and right by  $P^{-1}$ , and we define a new variable  $W = P^{-1}$ , then proposition 4.2 can be rewritten as follows.

**Proposition 4.3.** *The continuous fuzzy system (35) is quadratically stable for some feedback gain  $F_i$  if there exists a common positive definite matrix  $W$  such that*

$$\begin{aligned} A_i W + W A_i^T - B_i Y_i - Y_i^T B_i^T &< 0, \quad i = 1, \dots, r \\ A_i W + W A_i^T + A_j W + W A_j^T - B_i Y_j - Y_j^T B_i^T - B_j Y_i - Y_i^T B_j^T &\leq 0, \quad i < j \leq r \end{aligned} \quad (38)$$

being  $Y_i = F_i W$  so that for  $W > 0$ , we have  $F_i = Y_i W^{-1}$

Using these LMI conditions, we establish the first controller design constraint, next we describe the second design restriction.

As dc-dc converter control signal corresponds to the incremental duty cycle, then the control signal is bounded in the interval  $[-D, 1 - D]$ . In order to satisfy with this limitation, we constrain the control signal by the next proposition.

The satisfaction of the next proposition will assure that control signal  $d(t)$  is inside the interval  $[-D, 1 - D]$  from starting condition  $x(0)$  to the equilibrium point.

**Proposition 4.4.** Assume that initial condition  $x(0)$  is known. The constraint  $\|d(t)\|_2 \leq \mu$  is enforced at all times  $t \geq 0$  if the LMIs (39) hold

$$\begin{bmatrix} 1 & x(0)^T \\ x(0) & \mathbf{W} \end{bmatrix} \geq 0, \quad \begin{bmatrix} \mathbf{W} & \mathbf{Y}_i^T \\ \mathbf{Y}_i & \mu^2 \mathbf{I} \end{bmatrix} \geq 0 \quad (39)$$

where  $\mathbf{W} = \mathbf{P}^{-1}$  and  $\mathbf{Y}_i = \mathbf{F}_i \mathbf{W}$ .

Also, it will be desirable a suitable transient performances of the closed loop system. The entire fuzzy system transient performances depends on the localizations of the poles of its linear systems corresponding to each rule. In our case, this poles are expressed in terms of decay rate introduced via exponential stability, which it can be seen as a special case of pole-placement on the closed-loop system.

Consequently, we impose that this poles must be inside a predetermined region as the one pictured in Fig. 7. Therefore, the design process will add the next proposition, adapted from (Tanaka & Wang, 2001).

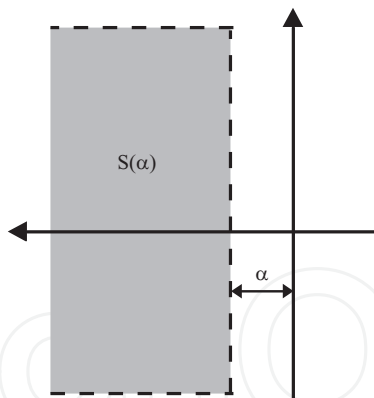


Fig. 7.  $S(\alpha)$  region

**Proposition 4.5.** The eigenvalues of  $(A_i - B_i F_j)$  in each linear fuzzy system are inside the region  $S(\alpha)$  if there exist a common positive definite matrix  $\mathbf{W}$  such that

$$A_i \mathbf{W} + \mathbf{W} A_i^T - B_i \mathbf{Y}_i - \mathbf{Y}_i^T B_i^T + 2\alpha \mathbf{W} < 0, \quad i = 1, \dots, r \quad (40)$$

$$A_i \mathbf{W} + \mathbf{W} A_i^T + A_j \mathbf{W} + \mathbf{W} A_j^T - B_i \mathbf{Y}_j - \mathbf{Y}_j^T B_i^T - B_j \mathbf{Y}_i - \mathbf{Y}_i^T B_j^T + 4\alpha \mathbf{W} \leq 0, \quad i < j \leq r$$

being  $\mathbf{F}_i = \mathbf{Y}_i \mathbf{W}^{-1}$ .

Between all the feasible set of feedback gains, the proposed algorithm finds the largest possible decay rate ( $\alpha$ ) of the state variables, satisfying the previous LMIs. Hence, the design procedure of the LMI Fuzzy control can be formulated by the following optimization algorithm.

$$\begin{aligned} & \max \quad \alpha \text{ subject to} \\ & \mathbf{W}, \mathbf{Y}_i \\ & i = 1, \dots, r \quad (39), \text{ and } (40) \end{aligned} \tag{41}$$

The solution of this optimization program with its corresponding LMIs will provide the set of feedback gains  $F_{LMI-Fuzzy} = \{F_1, F_2, F_3, F_4\}$ . The solution of this algorithm can be carried out by means of GEVP function in MATLAB LMI toolbox.

5. Design examples

This section shows two examples of LMI-based control applied to dc-dc converters. The first case presents the control design of a step-down converter working around equilibrium point. This example takes into account the same LMIs constraints of the algorithm (41). The second example proposes an LMI Fuzzy control for a step-up converter, allowing working at different operating point. Both examples are tested during a start-up and under load disturbances.

5.1 LMI control of a Buck converter

In this first example, we presents an LMI control approach applied to the problem of regulating the output voltage of the buck converter. The values of the converter parameter set are shown in Table 1. The nominal load of the converter is equal to 10  $\Omega$ , while supply voltage equal to 48 V. Consequently, the equilibrium point satisfying (7) is equal to  $[i_L \ v_C] = [4.8 \ 24]^T$ . The simulation prototype is designed to process less than 60 W corresponding to a load resistance  $R = 10 \ \Omega$ . The inductance and capacitance values and switching frequency have been selected to ensure low ripple level. In order to limit the control signal in the range  $[-D, 1 - D]$ ,  $\mu$  is set to 1500, since simulations show no saturation of the duty-cycle.

$V_g$	48V
$v_C(V_{ref})$	24V
$L$	200 $\mu H$
$C$	200 $\mu F$
$R$	10 $\Omega$
$D'$	0.5 $\Omega$
$T_s$	10 $\mu s$

Table 1. Buck converter parameters

Once the parameters values of the converter and controller have been defined, the next step is to obtain the feedback gain vector. Thus, solving the optimization algorithm (41) for the system (11), by means of the LMI toolbox of MATLAB (Gahinet et al., 1995), the state-feedback controller obtained for the buck converter is

$$\mathbf{F}_{Buck} = [0.0963 \ 0.1133 \ -319.8021]$$

with a decay rate of  $\alpha = 3254$ , which assures a maximum constant time of 1/3254, and consequently a maximum settling time of  $4 * (1/3254)$ . In order to verify the behavior of

the buck converter under the control law described above, numerical simulations have been carried out in MATLAB/Simulink, as shown in Fig.8.

Fig. 9 shows the transient simulation of the state variables and duty-cycle during start-up, in fact, represents a large signal perturbation around the equilibrium point of the state variables. It is remark that the settling time is smaller than 1.2 *ms*, and agrees with the decay rate obtained.

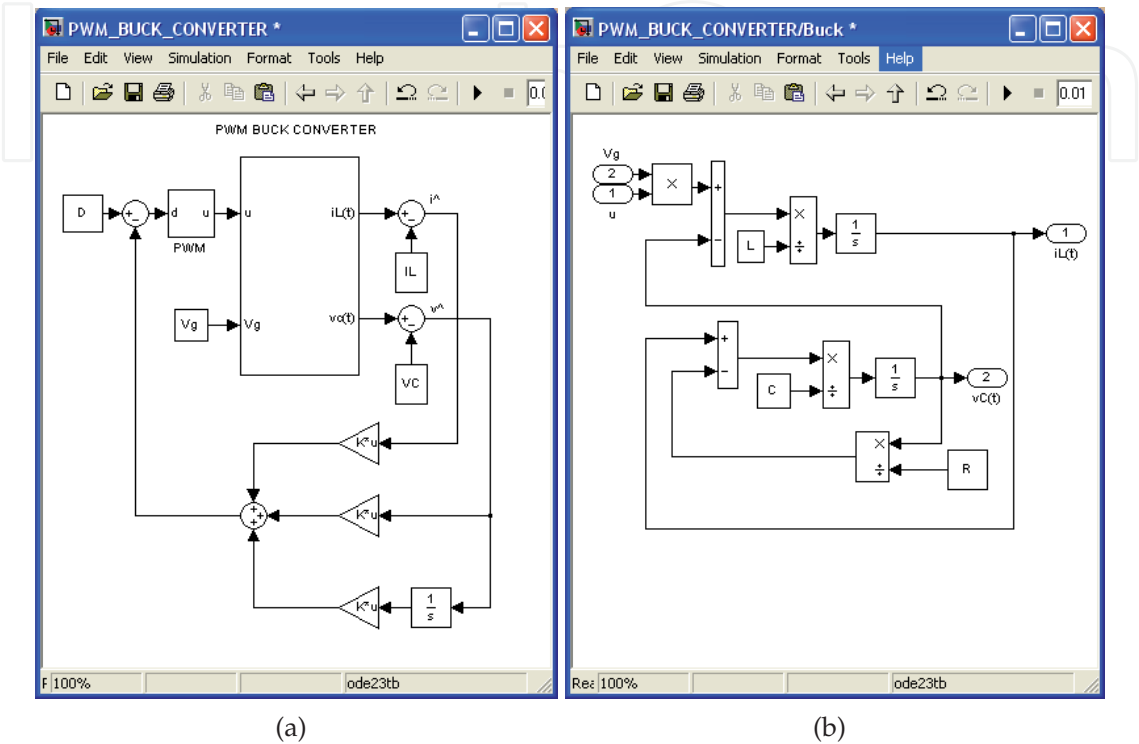


Fig. 8. Simulink diagram of a buck converter with state-feedback regulation. (a) Implementation diagram in MATLAB/Simulink. (b) Simulink model of the buck converter.

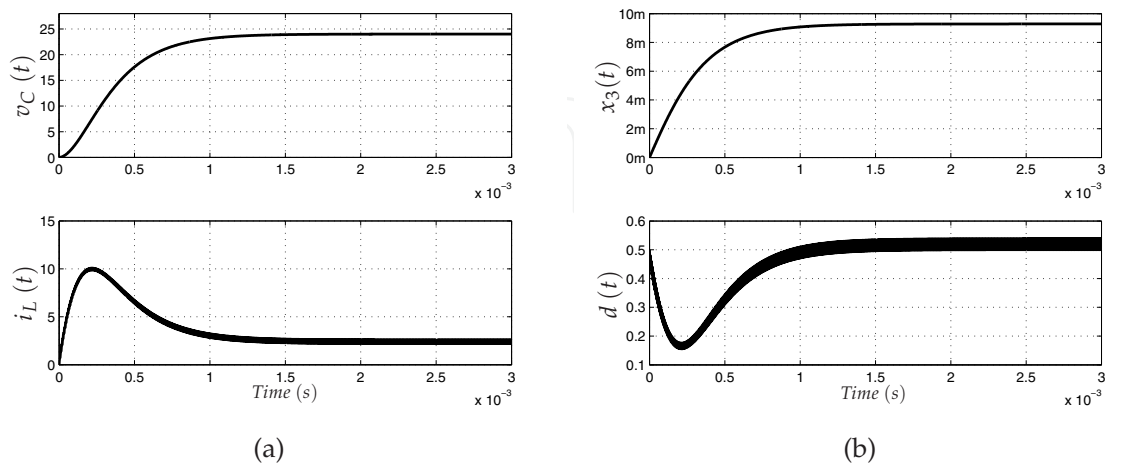


Fig. 9. Simulated response of the dc-dc buck converter during start-up. (a) Inductor current  $i_L(t)$  and capacitor voltage  $v_C(t)$ . (b) Steady-state error  $x_3(t)$  and duty-cycle  $d(t)$ .

Fig. 10 illustrates the system responses for step changes in the load current from 2.4 A to 4.4 A at 2ms and then returns to 2.4 A at 8ms. It can be observed that the controller regulates the output voltage  $v_C$  smoothly at 24 V after a short transient period. It can also be observed that the duty-cycle does not exceed the limits of interval  $[-D, 1 - D]$ . In the next subsection, the

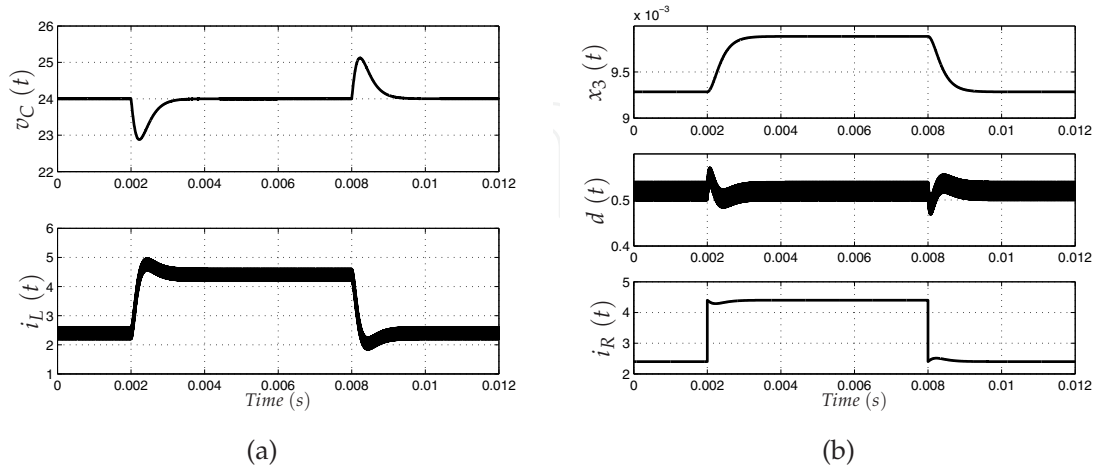


Fig. 10. Simulated response of the buck converter under a load step transient of 2 A. (a) Inductor current  $i_L(t)$  and capacitor voltage  $v_C(t)$ . (b) Steady-state error  $x_3(t)$ , duty-cycle  $d(t)$  and load current  $i_R$ .

LMI Fuzzy controller design for a boost converter is described.

5.2 LMI Fuzzy control of a boost converter

In this subsection, we present the results of the design of the LMI Fuzzy controller applied to fuzzy model of the boost converter shown in subsection 3.1, whose parameter set is shown in Table 2. Consequently, the equilibrium state is given by  $[i_L \ v_C] = [4.8 \ 24]^T$ .

The design of the control law consists of solving the optimization algorithm (41) for the

$V_g$	12V
$v_C(V_{ref})$	24V
$L$	300 $\mu H$
$C$	300 $\mu F$
$R$	10 $\Omega$
$D'$	0.5 $\Omega$
$T_s$	20 $\mu s$

Table 2. Boost converter parameters

four linear submodels of the fuzzy model. This submodels correspond to the vertices of the polytopic model of the boost converter in the region defined in Fig 6. Therefore, in order to ensure stability within the polytopic region during a start-up transition and disturbance, the polytopic region should be  $[\hat{i}_{min} = 0, \hat{i}_{max} = 20] \times [\hat{v}_{min} = 0, \hat{v}_{max} = 10]$ . To demonstrate the advantage of this Fuzzy approach, we will compare the LMI Fuzzy control with a LMI linear Control.

As in the previous subsection, the simulation prototype is designed to process less than 60 W, as well as the inductance and capacitance values and switching frequency are selected to ensure low ripple level. To maintain the control signal under the threshold limit value,  $\mu$  is set



to 350, for the two control designs. So, according to the optimization algorithm (41), the fuzzy state-feedback gains obtained via LMI Toolbox of Matlab are given follows:

$$\mathbf{F}_1 = [0.1737 \ 0.1019 \ -183.4507]$$

$$\mathbf{F}_2 = [0.2737 \ 0.1871 \ -313.9974]$$

$$\mathbf{F}_3 = [0.1814 \ 0.1157 \ -199.8689]$$

$$\mathbf{F}_4 = [0.1877 \ 0.1149 \ -202.6875]$$

The decay rate value obtained is 878, which assures a maximum settling time of  $4 * (1/878)$ . As mentioned above, to contrast the performance and robustness of the proposed control, we compare the LMI Fuzzy control law with a LMI linear law, which it presents the same optimization criteria (41). The resulting controller gain vector is

$$\mathbf{F}_{Boost} = [0.0895 \ 0.1018 \ -159.9759]$$

with a decay rate of 1950, that assures a maximum settling time of  $4 * (1/1950)$ .

It can be observed that there exist differences between the decay rate obtained above. Next, we will show its properties during a start-up and in presence of load disturbances. Fig. 11 shows the simulation schematic of the boost converter with the LMI Fuzzy controller implemented in MATLAB/Simulink. Note that the MATLAB Function block is used to run the LMI Fuzzy

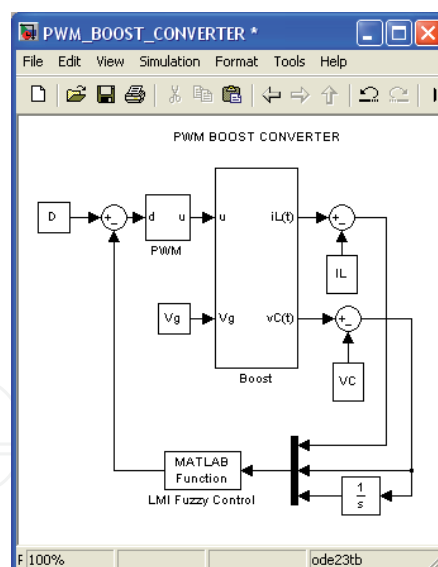


Fig. 11. Simulink implementation diagram of a boost converter with LMI Fuzzy regulation.

control on Simulink, which it is written by means of a code in the MATLAB Editor.

Fig. 12 illustrates the transient simulation of the boost converter during start-up. The waveforms depicted in the figure are the inductor current  $i_L$ , capacitor voltage  $v_C$ , steady-state error  $x_3$  and duty-cycle  $d(t)$ . The response of the LMI linear controller corresponds to dashed line, while the waveform of the LMI Fuzzy controller has been drawn with solid line. In Fig. 13, the converter reacts to large load disturbances. In this simulation the load current is initially 2.4 A. At  $t = 2 \text{ ms}$ , the current changes to 6.4 A, and at  $t = 8 \text{ ms}$ , it returns to its initial

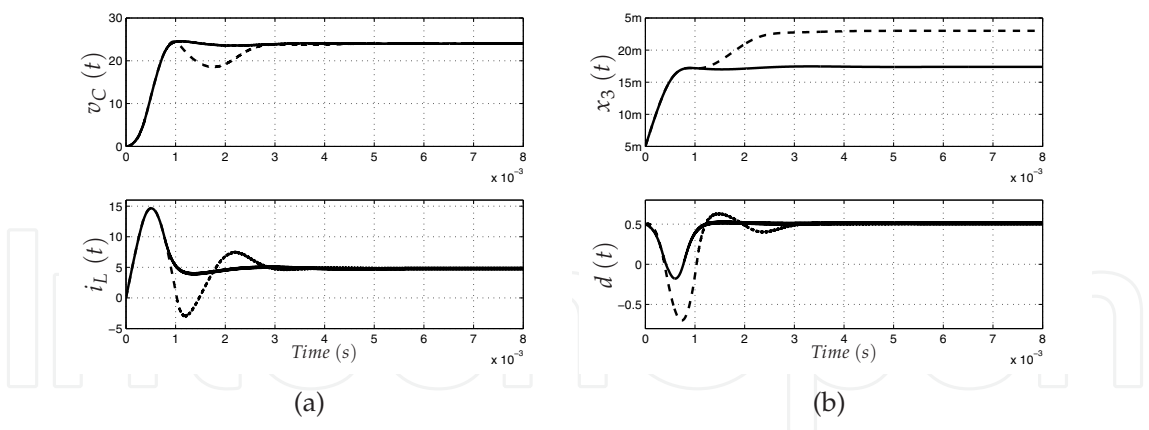


Fig. 12. Simulated responses of the dc-dc boost converter during start-up linearly controlled (dished) and fuzzy controlled (solid). (a) Inductor current  $i_L(t)$  and capacitor voltage  $v_C(t)$ . (b) Steady-state error  $x_3(t)$  and duty-cycle  $d(t)$ .

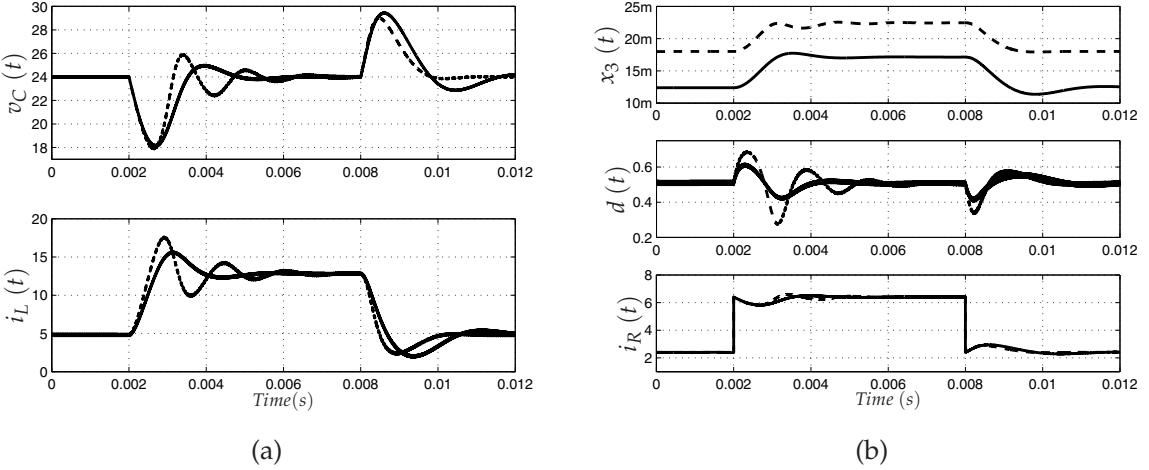


Fig. 13. Simulated responses of the boost converter under a load step transient of 4 A linearly controlled (dished) and fuzzy controlled (solid). (a) Inductor current  $i_L(t)$  and capacitor voltage  $v_C(t)$ . (b) Steady-state error  $x_3(t)$ , duty-cycle  $d(t)$  and load current  $i_R$ .

value. It is worth noting that state variables and duty-cycle are better with the LMI Fuzzy controller (dashed line), since it maintains its stability properties under large disturbances, and despite that it is slower. The main advantage of this controller, is that it ensures robust stability in broad range of operation.

## 6. Conclusions

This chapter presents a LMI fuzzy controller design for dc-dc converters using MATLAB. The design methodology has been applied to a buck converter and to a boost converter where the control optimizes the decay rate of the state variables subject to a bound in the control effort. The methodology allows us to take into account the bilinear nature of the boost converter dynamics. We express the control objective and the bound as LMIs. The set of LMIs, which is solved by means of LMI Toolbox, provides the feedback gains.

The dynamical performances of LMI fuzzy controlled boost converter have been compared those of a linear-controlled boost considering the same design constraint. We have verified the closed-loop dynamic behavior using Simulink/MATLAB. The plots exhibit a perfect agreement with the design specifications. This design procedure ensures the stability of the converter in a wide region. On the contrary, a linear-controlled converter deteriorates its performances out of the operating point. The approach can be extended to more complex converters or other types of bilinear plants.

## 7. Acknowledgment

This work was partially supported by the Spanish Ministerio de Educación y Ciencia under grant DPI2010-16481

## 8. References

- Boyd, S.; El Ghaoui, L.; Feron, E. & Balakrishnan, V. (1994). *Linear Matrix Inequalities in Systems and Control Theory*, ser. Studies in Applied and Numerical Mathematics, Philadelphia, PA:SIAM
- Chilali, M. & Gahinet, P. (1996).  $H_\infty$  Design with Pole Placement Constraints: An LMI Approach, *IEEE Trans. on Autom. Control.*, Vol. 42, No.3, (358-367)
- Driankov, D.; Hellendoorn, H. & Reinfrank, M. (1993). *An introduction to Fuzzy Control*, Springer-Verlag, Germany
- Erickson, R.W. & Macksimovic, D. (2001). *Fundamental of Power Electronics, Second ed.*, 920 pages, Kluwer Academic Publisher, ISBN 0-7923-7270-0, USA
- Gahinet, P.; Nemirovski, A.; Laub, A.J.; & Chilali, M. (1995). LMI Control Toolbox for Use With Matlab, *The MathWorks, Inc*, Vol. 3, No.1, (75-85)
- He, Y. & Luo, F.L. (2006). Sliding-mode control for dc-dc converters with constant switching frequency, *IEE Proc.-Control Theory Appl.*, Vol. 153, No.1, (37-45)
- Kawasaki, N.; Nomura, H. & Masuhiro, M. (1995). A new control law of bilinear DC-DC converters developed by direct application of Lyapunov, *IEEE Trans. Power Electron.*, Vol. 10, No.1, (318-325)
- Korba, P.; Babuska, R.; Verbruggen, H.B. & Frank, P.M. (2003). Fuzzy Gain Scheduling: Controller and Observer Design Based on Lyapunov Method and Convex Optimization, *IEEE Trans. on Fuzzy Syst.*, Vol. 11, No.3, (285-298)
- Kuang-Yow, L.; Jeih-Jang, L. & Chien-Yu, H. (2006). LMI-Based Integral Fuzzy Control of DC-DC Converters, *IEEE Trans. on Fuzzy Syst.*, Vol. 14, No.1, (71-80)
- Lan, H.K & Tan, S.C (2009). Stability analysis of fuzzy-model-based control systems: application on regulation of switching dc-dc converter, *IET Control Theory and Appl.*, Vol. 3, No.8, (1093-1106)
- Leyva, R.; Cid-Pastor, A.; Alonso, C.; Queinnec, I.; Tarbouriech, S. & Martínez-Salamero, L. (2001). Passivity-based integral control of a boost converter for large-signal stability, *IEE Proc.-Control Theory Appl.*, Vol. 153, No.2, (March) (139-146)
- Middlebrook, R. & Cuk, S. (1976). A general unified approach to modeling switching-converter power stages, in *IEEE Power Electron. Special. Conf.*, (June)(18-34), Cleveland
- Olalla, C.; Leyva, R.; El Aroudi, A. & Queinnec, I. (2009). Robust LQR Control for PWM Converters: An LMI Approach, *IEEE Trans. Ind. Electron.*, Vol. 56, No.7, (July) (2548-2558)

- Olalla, C.;Leyva, R.; El Aroudi, A.; Garcés, P. & Queinnec, I. (2009). Robust LQR Control for PWM Converters: An LMI Approach, *IET Power Electron.*, Vol. 3, No.1, (75-85)
- Sanders, S.R. & Verghese G.C.(1992). Lyapunov-based control for switched power converters, *IEEE Trans. Power Electron.*, Vol. 7, No.3, (17-24)
- Takagi, T. & Sugeno, M. (1985). Fuzzy Identification of Systems and Its Applications to Modeling and Control, *IEEE Trans. on Syst., Man, and Cyber.*, Vol. 15, No.1, (January) (116-132)
- Tanaka, K. & Wang, H.O. (2001). *Fuzzy Control Systems Design an Analysis*, Jhon Wiley & Sons, INC, New York
- Torres-Pinzón, C.A. & Leyva, R. (2009). Fuzzy Control in DC-DC Converters: an LMI Approach,in *Proc. of the IEEE Annual Conf. on Ind. Electron., IECON'09*, (November)(510-515),Porto

IntechOpen



## **MATLAB - A Ubiquitous Tool for the Practical Engineer**

Edited by Prof. Clara Ionescu

ISBN 978-953-307-907-3

Hard cover, 564 pages

**Publisher** InTech

**Published online** 13, October, 2011

**Published in print edition** October, 2011

A well-known statement says that the PID controller is the “bread and butter” of the control engineer. This is indeed true, from a scientific standpoint. However, nowadays, in the era of computer science, when the paper and pencil have been replaced by the keyboard and the display of computers, one may equally say that MATLAB is the “bread” in the above statement. MATLAB has become a de facto tool for the modern system engineer. This book is written for both engineering students, as well as for practicing engineers. The wide range of applications in which MATLAB is the working framework, shows that it is a powerful, comprehensive and easy-to-use environment for performing technical computations. The book includes various excellent applications in which MATLAB is employed: from pure algebraic computations to data acquisition in real-life experiments, from control strategies to image processing algorithms, from graphical user interface design for educational purposes to Simulink embedded systems.

### **How to reference**

In order to correctly reference this scholarly work, feel free to copy and paste the following:

Carlos Andrés Torres-Pinzón and Ramon Leyva (2011). MATLAB: A Systems Tool for Design of Fuzzy LMI Controller in DC-DC Converters, MATLAB - A Ubiquitous Tool for the Practical Engineer, Prof. Clara Ionescu (Ed.), ISBN: 978-953-307-907-3, InTech, Available from: <http://www.intechopen.com/books/matlab-a-ubiquitous-tool-for-the-practical-engineer/matlab-a-systems-tool-for-design-of-fuzzy-lmi-controller-in-dc-dc-converters>

**INTECH**  
open science | open minds

### **InTech Europe**

University Campus STeP Ri  
Slavka Krautzeka 83/A  
51000 Rijeka, Croatia  
Phone: +385 (51) 770 447  
Fax: +385 (51) 686 166  
[www.intechopen.com](http://www.intechopen.com)

### **InTech China**

Unit 405, Office Block, Hotel Equatorial Shanghai  
No.65, Yan An Road (West), Shanghai, 200040, China  
中国上海市延安西路65号上海国际贵都大饭店办公楼405单元  
Phone: +86-21-62489820  
Fax: +86-21-62489821

© 2011 The Author(s). Licensee IntechOpen. This is an open access article distributed under the terms of the [Creative Commons Attribution 3.0 License](https://creativecommons.org/licenses/by/3.0/), which permits unrestricted use, distribution, and reproduction in any medium, provided the original work is properly cited.

IntechOpen

IntechOpen